ARTICLE

Template Synthesis and Magnetic Behavior of FeNi Alloy Nanotube Arrays[†]

Dong Zhou*, Li-heng Cai, Fu-shen Wen, Fa-shen Li

Institute of Applied Magnetics, Key Laboratory for Magnetism and Magnetic Materials of the Ministry of Education, Lanzhou University, Lanzhou 730000, China

(Dated: Received on August 30, 2007; Accepted on October 10, 2007)

FeNi nanotubes were successfully prepared in pores of anodic aluminium oxide templates by the wetting template method. By varying the deposition conditions and the parameters of the templates, the lengths and the outer as well as the inner diameters of the tubes can be tailored. The FeNi nanotubes and their arrays were characterized by transmission and scanning electron microscopy. Macroscopic magnetic measurements show the FeNi nanotube arrays to have obvious anisotropy, and the easy axis is parallel to the nanotube axis. The magnetic moment distributions in the tube walls and the magnetization reversal mechanism are discussed. Magnetic moments of the FeNi nanotube preferentially lie in the nanotube wall, but the distribution is spatially isotropic. These magnetic behaviours are due to the unique shape of the nanotube.

Key words: Nanotube, Magnetic property, FeNi

I. INTRODUCTION

In recent years, nanostructures have been the intensely investigated fields of material [1-4]. An emerging area is the synthesis of tubular nanostructures, which is pioneered in inorganic chemistry [5]. Up to now, most researches on nanotubes have focused on carbon nanotubes [6-9]. Because of the development of the methods of preparing magnetic alloy nanotubes [10-13] and the potential applications of magnetic nanotubes in nanomedicine, biotechnology and ultrahigh-density magnetic storage devices [14-16], magnetic nanotubes have attracted more and more attention.

The methods for magnetic nanotubes fabrication include: electrodeposition [10], electroless deposition [11], pulsed laser deposition (PLD) technique [13], wetting templates technique [17] and so on. In this research, we improved the wetting template technique, by which we successfully synthesized a series of FeNi nanotube arrays in AAO templates. The advantages of this method in the production of magnetic and other inorganic nanotubes are obvious because of its convenience, simplicity, and capability of producing large quantities of samples. Among many kinds of magnetic materials, Fe-Ni alloys belong to the most important alloy systems in both basic magnetism and industrial applications due to their high saturation magnetization, high Curie temperature and other unique properties [18]. Researches about the fabrication and magnetic properties of FeNi nanotubes have produced few reports so far.

II. EXPERIMENTS

Aluminum foil (99.99%) was ultrasonically degreased in alcohol for 5 min, etched in 1.0 mol/L sodium hydroxide at room temperature for 3 min to remove the native oxide and washed thoroughly with distilled water, then electropolished in a mixed solution of perchloric acid and alcohol (1:4, V/V) for 20 s and promptly rinsed with distilled water. After that the anodic aluminum oxide template with pore diameter of about 200 nm was prepared by anodic oxidation of the obtained aluminum foil in phosphoric acid under a two-step anodizing process [19]. The first process was carried out at a constant voltage of 120 V in 0.3 mol/L H_3PO_4 solution at room temperature for 1 h. Secondly, the oxide film was dissolved in 0.4 mol/L H_3PO_4, 0.2 mol/L $H_2Cr_2O_4$ at 60 °C. After that the anodization was performed for 3 h under the same conditions as the first step. By varying the anodization conditions, the pore diameter, spacing, and depth can be tuned and also the pore ordering can be controlled [20-23].

FeNi nanotube arrays were fabricated according to the following steps: Step 1. The as-prepared templates were dipped into a solution of $Fe(NO_3)_3{\cdot}9H_2O$ and $Ni(NO_3)_2{\cdot}6H_2O$ having a Fe:Ni atomic ratio of 2:1. Step 2. The loaded templates were cleaned and then fixed on a sample holder, with pores mounted horizontally, and dried in an oven at 60 °C for more than 10 h. Then a thin Ni/Fe nitrate film covered the pore wall. Step 3. The templates were placed in an oven for 3 h at 400 °C for the metal salts decomposition. Step 4. The samples were put into an oven with flowing hydrogen for 5 h at 400 °C to form FeNi nanotube arrays. Steps 1-3 can be called dip-coating procedure, which can be repeated again and again, so the thickness and quality of tube wall can be changed. By varying the number of dips from 1 to 6, samples with different tube wall thickness were prepared. According to the numbers of dips

[†]Part of the special issue from "The 6th China International Conference on Nanoscience and Technology, Chengdu (2007)".

*Author to whom correspondence should be addressed. E-mail: zhoud03@lzu.cn

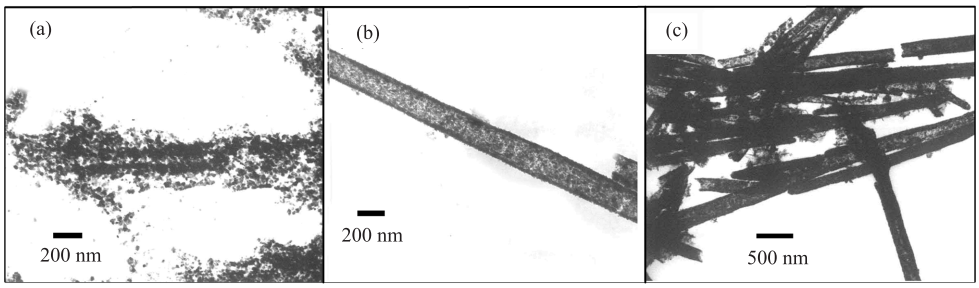

FIG. 1 TEM images of FeNi nanotubes (a) D1, (b) D4, and (c) D6.

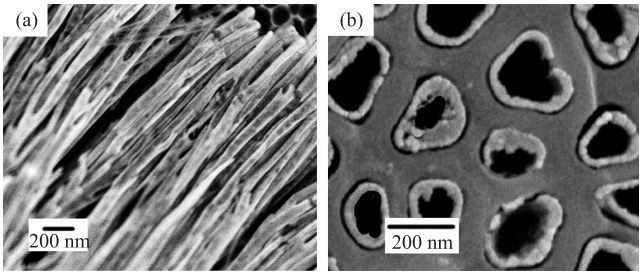

FIG. 2 SEM images of D4 (a) view from the top; (b) view from the side.

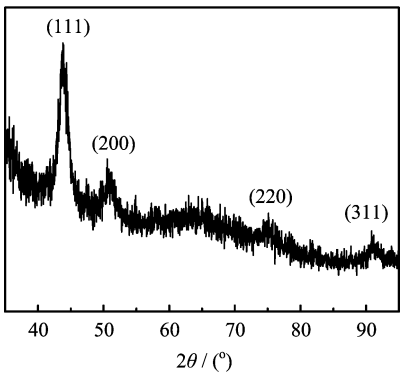

FIG. 3 XRD pattern of FeNi nanotube array with AAO template.

in the dip-coating procedure, the samples were named from D1 to D6, respectively.

Transmission electron microscopy (TEM, Hitachi S-4800, Japan) and scanning electron microscopy (SEM, Hitachi 600, Japan) were used to confirm the morphology of the FeNi alloy nanotubes. The crystalline structures of the samples were obtained by X-ray diffractometer (Philips x'pert, Holland). Macroscopic magnetic properties were measured by a vibrating sample magnetometer (Lakeshore 7304, USA) at room temperature. ^{57}Fe Mössbauer spectrum was taken at room temperature with a transmission geometry equipped with ^{57}Co (Pd). Using α-Fe to calibrate the driver velocity, the spectra parameters were calculated by fitting Lorentzian line shapes to the experimental data using the least-squares method.

III. RESULTS AND DISCUSSION

Figure 1 shows the TEM images of FeNi nanotubes released from alumina. As can be seen from Fig.1(a), the coupling of the tube wall of D1 is loose. Figure 1(b) shows the D4 sample, from which we can see that the coupling of the tube wall is compact. Figure 1(c) shows the image of D6. It can be seen that with the increase of the repeating times, the quality of the tubes is improved and the thickness of the tube wall is increased.

For convenience of the fabrication, four times of the dip-coating procedure will be a good choice. Figure 2 shows the SEM images of D4. According to Fig.2(b), each hole just hosts one nanotube, so that the morphology of the nanotube is defined by the internal shape of the hole and the overall density of the nanotube in the template is determined by the density of the holes. Figure 3 shows the XRD pattern of D4, which reveals that the crystal structure of FeCo alloy is a face-centered cubic.

Magnetic measurements of the prepared FeNi nanotube arrays are performed at room temperature using the VSM without demagnetization corrections. In order to investigate the effect of number of dips on macroscopic magnetic properties, the variations of coercivity and squareness ratio with the dipping number are given in Fig.4 respectively, from which we can find that the coercivity and the squareness ratio measured out of plane are always larger than in plane. Because of the unique shape anisotropy, the sample can be magnetized more easily when the field applied is parallel to the axis of the nanotubes. If the magnetization direction is along the tube axis, the energy barrier should be jump over when magnetization reversal will be higher than the case when the direction is in plane, so the coercivities measured out of plane have higher values.

As can be seen from Fig.4, the coercivities increase before 4 dips, and after that they basically remain the same. The squareness ratios of the samples increases at first, then they decrease after 4 dips when the field is applied parallel to the tube axis. In contrast, they keep

DOI:10.1088/1674-0068/20/06/821-825

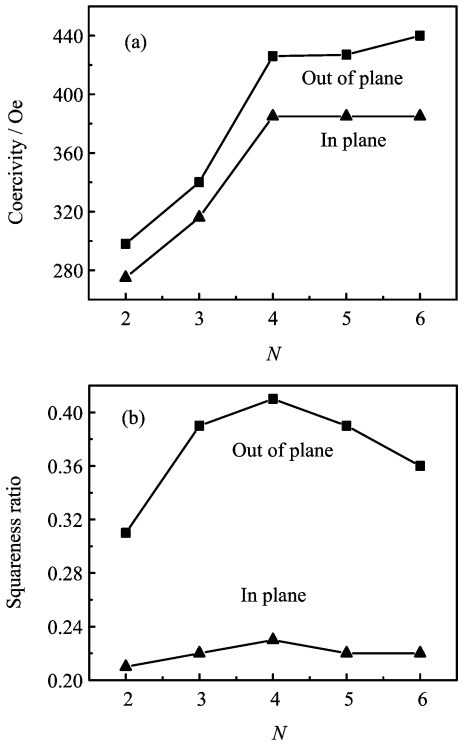

FIG. 4 The number of dips dependence of (a) the H_c of the nanotube arrays and (b) the squareness ratio of the nanotube arrays.

nearly unchanged when the field is applied perpendicular to the tube axis. The variations of coercivities and squareness ratios shown in Fig.4 may be related to surface effect. Because of the reduced coordination and broken exchange bonds between surface spins, generally the surface spin of magnetic nanomaterial is disordered [24]. With the increase of the tube wall thickness, the surface ratio of nanotube will decrease and the quality of the tube wall will be improved. At the same time, the effect on the magnetic properties arising from the surface and interface decrease, so the coercivities of the samples increase.

Although the magnetization reversal process is well known for ferromagnetic nanowires, the equivalent phenomenon in nanotubes has been poorly explored in spite of some potential advantages over solid cylinders [25]. It is important to understand the method and conditions for reversing the orientation of the magnetization. The basic mechanisms of magnetization reversal of magnetic nanotubes are coherent rotation mode and curling mode. Like in other nanostructures, such as nanospheres and nanowires, there is a transition from coherent rotation to curling when the radius R exceeds a certain value. However, in nanotubes, this transition occurs at a very small tube radius R. Since the nanotubes considered have a radius of about 50 nm, coherent rotation can safely be ruled out [5]. The diameter of the nanotubes fabricated in the experiment is about 200 nm, so the reversal mechanism is curling mode. The curling mode can be divided into two sub-modes when discussing the magnetization reversal mechanism of magnetic nanotube, which depends on the internal radius r and external radius R as well as the magnetocrystalline anisotropy of the magnetic material [5,25]. The sub-modes are vortex wall, where spins rotate progressively via propagation of a vortex domain; and transverse wall, where spins rotate progressively via propagation of a transverse domain wall. When discussing the curling mode in magnetic nanotubes, an issue is polycrystallinity, which may distort the curling character of the reversal mode. The transition between the vortex wall mode and the transverse wall mode occurs at some radius $R_{\rm rand}$ that depends on the magnetocrystalline anisotropy. Applying standard random anisotropy analysis to the problem yields [5]

$$R_{\rm rand} \approx \frac{{\delta_B}^2 t^{1/2}}{a^{3/2}} \tag{1}$$

where a is the polycrystalline grain size and $\delta_{B\sim}(A/|K_1|)^{1/2}$ is the Bloch-wall thickness of the corresponding bulk material. Because of the low value of K_1 of FeNi alloy, the reversal in the FeNi tubes is vortex wall mode.

The curling mode is also affected by the ratio of r/R. In this experiment, the value of r/R nearly equals 0.8. According to simulation, when the value is more than 0.5, the reversal process is always vortex wall [25]. For each value of the r/R, there exists a critical radius $R_c(r/R)$ at which both energy barriers of vortex wall and transverse wall are equal. For $R<R_c(r/R)$, the tube reverses its magnetization creating a transverse wall, while for $R>R_c(r/R)$, a vortex wall appears. The $R_c(0.8)$ of the FeNi nanotube calculated by Landeros *et al.* is about 7 nm [25], which is much smaller than the radius of FeNi nanotube used in this experiment, so the tube reverses its magnetization creating a vortex wall.

All of the discussion mentioned above shows that the magnetization reversal mechanism of the FeNi nanotube is vortex wall mode, however the defects in the nanotubes and the surface effect make the reversal process complex and difficult to predict.

Compared with the one-dimensional (1D) nanowire and two-dimensional (2D) film, the quasi-1D nanotube has its own unique magnetic properties. For one-dimensional magnetic nanowire, the demagnetization field tends to align the magnetic moments along the axis of the nanowire, which has been confirmed for Fe and FeCo alloy nanowire arrays by transmission Mössbauer spectroscopy [26]. For 2D thin magnetic film, the demagnetization field tends to push down the magnetic moments in the plane [27]. As a 1D material, a nanotube has a more particular shape. Understanding of the static distribution of magnetic moments in nanotubes is the basis for further study of the magnetic behaviours. The distribution of the magnetic moments in the nanotubes depends on the competition between

DOI:10.1088/1674-0068/20/06/821-825

magnetocrystalline anisotropy energy (E_k) and demagnetization energy (E_d). Because of the unique shape of the nanotube, the tube can be considered like a magnetic film which is rolled up to form a tube. This can be understood from another explicit method: if an FeNi tube is imagined to be unfolded to a thin film, the magnetic moments preferentially lie in the plane.

It is well known that the FeNi alloy has very low magnetocrystalline anisotropy energy, so the demagnetization field in the tube wall tends to push down the magnetic moments in the plane of the film. To further the study of magnetic moment distribution in nanotubes, the room temperature transmission Mössbauer spectrum of the sample was determined (Fig.5). In the transmission geometry, the incident γ photons are parallel to the long axis of nanotubes (perpendicular to the membrane). The experimental data are fitted by a magnetic splitting sextet and a paramagnetic doublet. The doublet can be induced by two possible factors. One is spin disorder in the surface due to a large surface ratio, the other is the superparamagnetic phase resulting from the small particles in the polycrystalline nanotube array.

In the Mössbauer spectrum, the intensity ratio of 2, 5 peaks and 1, 6 peaks ($I_{2,5}/I_{1,6}$) depends on the angle between the γ beam and magnetic moments in the sample, and can be written as:

$$\frac{I_{2,5}}{I_{1,6}} = \frac{4\sin^2\theta}{3(1+\cos^2\theta)} \tag{2}$$

When θ=0°, the intensity ratio $I_{2,5}/I_{1,6}$ is 0, and $I_{2,5}/I_{1,6}$ is 4/3 when θ=90°. If the distribution of magnetic moments is spatially isotropic, $I_{2,5}/I_{1,6}$ is 2/3 [27]. From Fig.4, the relative intensity ratios of the 2, 5 and 1, 6 peaks is about 2/3, which suggests that, with respect to the tube axis direction, the magnetic moment distributions are approximately spatially isotropic. Combining with the unique shape anisotropy of the nanotube and the film conjecture mentioned above, the magnetic moment distribution configuration in FeNi nanotubes can be suggested. That is it is like a magnetic film, but it is rolled up to form a tube. The magnetic moments lie only in the tube walls, while in the plane of the tube wall, the distribution of the magnetic moments is isotropic. We also find the same phenomena in FeCo alloy nanotube array [28].

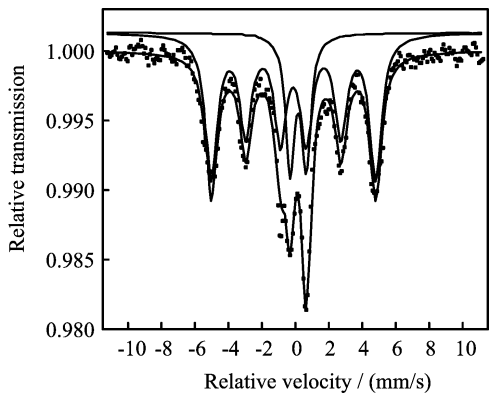

FIG. 5 Room temperature transmission Mössbauer spectrum of D4 with 200 nm in diameter and 25 nm in wall thickness. The solid line is the fitting curve.

IV. CONCLUSION

In summary, a series of FeNi nanotube arrays were fabricated. By controlling the experimental conditions, the diameter and length of the nanotubes, and the thickness as well as the quality of the tube wall can be changed. Magnetization measurements on the arrays of FeNi nanotubes demonstrate a perpendicular magnetic anisotropy, which is mainly attributed to shape anisotropy. With the increase of tube wall thickness, the coercivity increases at first, then it basically remains the same. This may stem from the improvement of the tube wall quality and the decrease of the surface atom ratio. The magnetic moment distribution configuration in FeNi nanotubes is suggested: it is like a magnetic film, but it is rolled up to form a tube. The magnetic moments lie only in the tube walls, while in the plane of the tube wall, the distribution of the magnetic moments is isotropic.

V. ACKNOWLEDGMENT

This work was supported by the National Natural Science Foundation of China (No.90505007).

[1] W. Q. Han, L. J. Wu, Y. M. Zhu, and M. Strongin, Nano Lett. **5**, 1419 (2005).
[2] Y. D. Yang, Z. W. Song, and Y. Lang, Chin. J. Chem. Phys. **18**, 605 (2005).
[3] Q. F. Zhan, Z. Y. Chen, D. S. Xue, and F. S. Li, Phys. Rev. B **66**, 134436 (2002).
[4] J. J. Mallett, E. B. Svedberg, M. D. Vaudin, L. A. Bendersky, A. J. Shapiro, W. F. Egelhoff, and T. P. Moffat, Phys. Rev. B **75**, 085304 (2007).
[5] Y. C. Sui, R. Skomski, K. D. Sorge, and D. J. Sellmyer, Appl. Phys. Lett. 84, 1525 (2004).
[6] H. H. Yu, D. S. Yu, L. D. Zhou, H. X. Wang, and D. S. Jiang, Chin. J. Chem. Phys. **18**, 1039 (2005).
[7] S. Glenis, V. Likodimos, N. Guskos, and C. L. Lin, J. Magn. Magn. Mater. **272-276**, 1660 (2004).
[8] C. A. Macedo and A. M. C. Souza, Physica B **354**, 290 (2004).
[9] Z. K. Tang, H. D. Sun, J. Wang, J. Chen, and G. Li, Appl. Phys. Lett. **73**, 2287 (1998)
[10] J. C. Bao, C. Y. Tie, Z. Xu, Q. F. Zhou, D. Shen, and Q. Ma, Adv. Mater. **13**, 1631 (2001).

DOI:10.1088/1674-0068/20/06/821-825

[11] S. C. Lin, S. Y. Chen, S. Y. Cheng, and J. C. Lin, Solid State Sci. **7**, 896 (2005).
[12] K. Nielsch, F. J. Castao, S. Matthias, W. Lee, and C. A. Ross, Adv. Eng. Mater. **7**, 217 (2005).
[13] Z. Q. Liu, D. H. Zhang, S. Han, C. Li, B. Lei, W. G. Lu, J. Y. Fang, and C.W. Zhou, J. Am. Chem. Soc. **127**, 6 (2005).
[14] S. Khizroev, M. H. Kryder, D. Litvinov, and D. A. Thompson, Appl. Phys. Lett. **81**, 2256 (2002).
[15] R. Gasparac, P. Kohli, M. O. Mota, L. Trofin, and C. R. Martin, Nano Lett. **4**, 513 (2004).
[16] C. A. Haberzettl, Nanotechnology **13**, 9 (2002).
[17] M. Steinhart, J. H. Wendorff, A. Greiner, R. B. Wehrspohn, K. Nielsch, J. Schilling, J. Choi, and U. Gösele, Science **296**, 1997 (2002).
[18] Y. Nakamura, Hyperfine Interact **83**, 55 (1994).
[19] S. G. Yang, H. Zhu, D. L. Yu, Z. Q. Jin, S. L. Tang, and Y. W. Du, J. Magn. Magn. Mater. **222**, 97 (2000).
[20] A. P. Li, F. Muller, A. Birner, K. Nielsch, and U. Gosele, J. Appl. Phys. **84**, 6023 (1998).
[21] O. Jessensky, F. Muller, and U. Gosele, Appl. Phys. Lett. **72**, 1173 (1998).
[22] H. Masuda and K. Fukuda, Science **268**, 1466 (1995).
[23] H. Masuda, H. Yamada, M. Satoh, H. Asoh, and M. Nakao, Appl. Phys. Lett. **71**, 2770 (1997).
[24] R. H. Kodama, A. E. Berkowitz, E. J. Jr. McNiff, and S. Foner, Phys. Rev. Lett. **77**, 394 (1996).
[25] P. Landeros, S. Allende, J. Escrig, E. Salcedo, and D. Altbir, Appl. Phys. Lett. **90**, 102501 (2007).
[26] F. S. Li, L. Y. Ren, Z. P. Niu, H. X. Wang, and T. Wang, Sci. China, Ser. B: Chem. **46**, 90 (2003).
[27] M. Kopcewicz, T. Lucinski, F. Stobiecki, and G. Reiss, J. Appl. Phys. **85**, 5039 (1999).
[28] F. S. Li, D. Zhou, T. Wang, Y. Wang, L. J. Song, and C. T. Xu, J. Appl. Phys. **101**, 014309 (2007).

DOI:10.1088/1674-0068/20/06/821-825